

## ALUMINIZING AS A METHOD OF IMPROVEMENT OF MAR-M247 ALLOY LIFETIME

M. Zagula-Yavorska

Rzeszów University of Technology, Department of Materials Science, Faculty of Mechanical Engineering and Aeronautics, Rzeszów, Poland

(Received 22 April 2024; Accepted 07 June 2024)

### Abstract

Environmentally friendly high temperature high-activity (HTHA) and high temperature low- activity (HTLA) CVD aluminizing processes were realized on the Mar-M247 heat resistant superalloy substrate that is widely used in the hot section of aircraft engines. Additionally, commercial aluminide coatings deposited in the above-the-pack aluminizing process were analyzed. The aluminizing of the Mar-M247 superalloy by the HTHA, HTLA and above-the-pack processes led to formation of two layers of the coatings. The outer layer of the coatings formed by the above-the-pack process consisted of the  $\beta$ -NiAl phase with precipitates, while the outer layer of coatings formed by the HTHA and HTLA processes consisted of the pure  $\beta$ -NiAl phase. Aluminizing successfully improved the lifetime of Mar-M247 superalloy. Despite the fact that the coatings formed by the above-the-pack process are thicker and have a higher aluminium concentration than the coatings formed by the HTLA aluminizing and process, the lifetime of the coated superalloy was lower. Moreover the oxidation resistance of the coated superalloy in the HTLA aluminizing process was better than that of the coating in the HTHA aluminizing process. The removal of impurities in the HTLA aluminizing process ensured a "pure" outer layer of the coatings. Clean aluminide coatings may create a purer alumina oxide and may prolong its lifetime.

**Keywords:** HTLA process; HTHA process; Above-the-pack process; Lifetime

### 1. Introduction

Nickel based alloys exhibit high strength and also this maintain strength over a wide temperature range, superalloys [1]. Precipitates of the ordered  $\text{Ni}_3\text{Al}$  intermetallic compound known as  $\gamma'$ , ensure the main mechanism for strengthening of superalloys. Further strengthening is achieved by  $\gamma$  solid solutions of alloying elements in nickel and precipitates of carbide [2]. The nickel sites in the  $\gamma'$  structure may contain cobalt, chromium and molybdenum, while the aluminum sites may contain titanium and niobium [3]. The  $\gamma'$  structure is coherent with the  $\gamma$  solid solution matrix. The precipitates of the  $\gamma'$  phase have a low driving force for size growth. Small precipitates hinder the movement of dislocations, resulting in a significant increase in strength. Polycrystalline nickel based superalloys used as rotating turbine blades, tend to fail at grain boundaries that versed transversely to the centrifugal force along axis of the blade [4]. The failure may be significantly limited by eliminating grain boundaries that are transverse to the centrifugal force [5]. The elimination of transverse grain boundaries is achieved through directional solidification [6]. The creep properties may be improved by eliminating grain boundaries of the

superalloys [7]. This is achieved by using a grain selector. Aluminum and chromium in the chemical composition of the superalloy improve its oxidation and corrosion resistance. However, beyond certain content these elements diminish creep strength of the superalloy [8]. The creep strength is achieved by the heat treatment of the superalloy, while the oxidation and corrosion resistance is improved by the deposition of metallic coatings with the proper aluminum and chromium content on the surface of the superalloy [8-9]. A thin oxide layer is formed on the metallic coatings surface in the oxidizing gases environment [10-11]. A number of requirements have to be satisfied in order to extend the protection of the coated superalloy [8,12]. The protective oxides on the coated superalloy surface should be thermodynamically stable and have a uniform thickness. Moreover, a slow growth rate of the oxide and good adhesion to the coating are required as well as a high concentration of the forming elements are needed. A protective alumina oxide forms on the surface of aluminide diffusion coatings during its high temperature exposure in the air [8,13-15]. There are three main processes in which aluminide diffusion coating can be formed [8]. There are: 1) pack, 2) above-the-pack and 3) chemical vapor deposition (CVD) processes. One

Corresponding author: yavorska@prz.edu.pl

<https://doi.org/10.2298/JMMB240422014Z>



of the stages which is common in three processes is formation of aluminum containing vapors [16]. The aluminum containing vapors are transported to the substrate and react with superalloy constituents and aluminide coating is being formed.

The elements to be coated in pack process are cleaned by grit blasting with alumina grits, whereas the area of the elements to be uncoated is masked. The masked elements are placed in a pack mix in a sealed or semisealed retort. The retort is placed in a furnace and heated at 800-1000 °C in the hydrogen or argon atmosphere [17]. The pack mix composes with the source of aluminum, activator (NaCl, NH<sub>4</sub>Cl or CrF<sub>2</sub>) and alumina powder, the so-called "inert constituent". The inert alumina powder prevents sintering of the pack mix [3,18]. The aluminum halide vapors form as a result of a halide activator reaction with the source of aluminum. The low costs and good coating reproducibility are advantages of the pack process. However, the frequent pack particles entrapment in the coating and the limited coating thickness are disadvantages of the pack process. The coatings are applied commercially by Pratt & Whitney, Chromalloy, General Electric and Rolls Royce gas turbine engines manufacturers [8].

The elements to be coated in the above-the-pack process are positioned inside the retort, but without contact with the pack [19]. The coating formation process includes several stages: the aluminum chlorides vapor formation; the transport of the aluminum chlorides vapor to the substrate; the deposition of aluminum at the surface of the substrate; the coating formation by the aluminum diffusion into the substrate and the substrate elements' diffusion into the surface. The vapors have access to both internal and external surfaces of the elements to be coated. The uniform coating thickness on the surface of the turbine blades and inside their cooling channels as well as a clean coatings, without entrapment of pack particles, are advantages of the above-the-pack process. The coatings are applied commercially by the above-the-pack process, among others, by Pratt & Whitney, Turbine Component Corporation and SIFCO gas turbine engines manufacturers [8].

The elements to be coated in the chemical vapor deposition process are inserted in a retort. The retort with the elements is kept in a furnace at 1000-1100 °C [20]. The halide vapor is formed in external gas generator as a result of hydrochloride passing over aluminum pellets at about 300 °C. The generator is separated from the retort containing the elements to be coated [21]. The chemical vapor deposition process has several advantages in comparison to the pack and above-the-pack processes [8,22]. The deposition rate can be controlled independently, and heat treatment of the superalloy after coating deposition can be performed without removing elements, which reduces

processing cost. In addition, a controlled, uniform coating thickness on the surface of the turbine blades and inside their cooling channels can be obtained. The coatings are applied commercially using the chemical vapor deposition process including by the Howmet gas turbine engine manufacturer [8].

The process is called 1) "low activity" or 2) "high activity" depending on the temperature of the process and the aluminum content in the pack [23]. 1) While the activity of the aluminum is low and the temperature is > 1000 °C, nickel diffuses out of and combines with aluminum to form  $\beta$ -NiAl external zone. The internal zone called the interdiffusion zone, loses nickel. The low solubility of the alloying constituents of the superalloy in the  $\beta$ -NiAl phase leads to the precipitation in the internal zone. The low activity aluminide coating appears to have two zones (external and interdiffusion). The  $\beta$ -NiAl phase is located in both zones.

2) While the activity of aluminum is high and the temperature is < 950 °C aluminum diffuses inward of the superalloy [24]. The inward aluminum diffusion is higher than outward nickel diffusion and the original surface of superalloy becomes the surface of the coating. The coating's phase composition depends on the activity of aluminum. Very high aluminum activity ensures formation of the  $\delta$ -Ni<sub>2</sub>Al<sub>3</sub> phase [8,25]. High aluminum activity ensures formation of the  $\delta$ -Ni<sub>2</sub>Al<sub>3</sub> phase in the external zone with the adjacent  $\beta$ -NiAl phase. Moderate aluminum activity ensures formation of the  $\beta$ -NiAl phase over the coating. The additional heat treatment is required to convert the  $\delta$ -Ni<sub>2</sub>Al<sub>3</sub> brittle phase into the less brittle phase Al-rich (> 50 at.%)  $\beta$ -NiAl. Aluminum diffuses inwards in the upper third of the coating, whereas nickel diffuses outwards in the bottom third of coating. Connection of the nickel that moves out of the interdiffusion zone with aluminum, that moves in from the outer zone result in the  $\beta$ -NiAl phase formation in the middle zone of the coating. The thickness of the coating increases roughly as the square root of the process time at the aluminizing temperature [8].

Aluminizing performed by the pack cementation or above-the-pack processes meets the technological criteria required in the production of aircraft engines. However, volatile chlorides are formed during pack cementation or above-the-pack aluminizing and cause environmental pollution. Currently, General Electric, Pratt & Whitney or Rolls-Royce – the worlds largest manufacturers of aircraft engines are currently looking for an aluminide coating manufacturing process that is environmentally friendly and allows producing a coating on the surface of the internal cooling channels of the turbine blades of aircraft engines. These criteria meet the chemical vapour deposition aluminizing process. Volatile chlorides are neutralized by the gas neutralization system. Lifetime

of coatings is the result of a well performed aluminizing process. An incorrectly performed aluminizing process does not provide protection from oxidation and shortens coated superalloy lifetime. Unfortunately, the data on these processes has not been clarified in the literature, and is closely guarded by aircraft engines manufacturers.

Therefore, a high temperature low-activity (HTLA) or high temperature high-activity (HTHA) CVD environmentally friendly aluminizing processes were carried out. Additionally, commercial aluminide coatings deposited in the above-the-pack aluminizing process were analyzed. The Mar-M247 heat resistant superalloy was taken as a substrate since it is used in the hot section of aircraft engines. The effects of the aluminizing processes on the microstructure, chemical composition, phase composition and oxidation resistance of the coated superalloy were performed. Moreover, the lifetime of the coated superalloy was compared to the uncoated one. The available experimental data about it are insufficient.

## 2. Experimental

The Mar-M247 (polycrystalline) Ni-based superalloy was used as a substrate. The chemical composition of superalloy is given in Table 1.

The circular samples, 14 mm diameter and 4 mm high were used. The samples of the superalloy were cut from the rod, than ground with the sandpapers of the following grit: 220, 500 and 1000. The ground samples were ultrasonically cleaned in ethanol and then dried with the compressed air.

A high temperature low-activity (HTLA) or high temperature high-activity (HTHA) CVD environmentally friendly aluminizing processes were carried out. The  $AlCl_3$  gas atmosphere during the HTLA process was created in an external reactor by passing hydrogen chloride HCl through the generator heated to approx. 350 °C which contained aluminum with a purity of 99.999 at. % (Fig.1a). Subsequently,  $AlCl_3$  gas was transported by hydrogen into the retort with samples heated up to 1050 °C. The process was performed at 1050 °C for 12 h. The activity of the aluminum was increased by using Al-Cr powder inside the retort (Fig. 1b-d Table 2). The post-process gases were passed through the gas neutralization system. Hence, these processes meet manufacturers' environmental protection requirements. Additionally, commercial aluminide coatings deposited in the above-the-pack aluminizing process were analyzed.

The aluminized samples were cut, ground and polished according to the ASTM E3 [26]. The cross-section microstructure of the coatings was examined

**Table 1.** Chemical composition of Mar-M247 superalloy, wt. %

C	Cr	Co	Al	Mo	W	Ti	Fe	Ta	B	Zr	Hf	Ni
0.15	8.25	10	5.5	0.7	10	1	0.5	3	0.015	0.005	1.5	59.38

**Table 2.** Chemical composition of the Al-Cr powder

Elements content			
wt. %		at. %	
Al	Cr	Al	Cr
40.8	59.2	57	43

by an Nikon Epiphot 300 optical microscope, a Hitachi S-3400N scanning electron microscope and an energy dispersive spectroscope according to ASTM B487 [27]. The thickness of the coatings was measured using the NIS-Elements software. ARL X'TRA X-ray diffractometer with a filtered copper lamp was used to investigate the crystal structure of the coatings. Oxidation resistance was investigated in the air atmosphere. An oxidation cycle included 20 h heating in air at 1100 °C and subsequent cooling to the room temperature. The mass changes were measured with an accuracy of  $10^{-5}$  g using an electronic balance. The oxidation test duration was 1000 h.

## 3. Results and Discussion

### 3.1. Effect of aluminizing processes on the microstructure, chemical and phase composition of coatings

The cross-section of the coating formed in the HTHA process is shown in Fig. 2a. Two layers were identified: the outer (A and B) and the interdiffusion one (C). The outer layer is a hyper-stoichiometric nickel-rich  $\beta$ -NiAl phase. The Al content is 45.5 at. % and the Ni content is 51.0 at. % at a distance from the surface 3-5  $\mu$ m (A) was found (Fig. 2-3a, Table 3). While the Al content 34.5 at. % and the Ni content 52.1 at. % at a distance from the surface 16-17  $\mu$ m (B) was proved. Moreover, the alloying elements (Cr, Co and W), that diffused from the substrate were in solution. Beneath the outer layer the interdiffusion one was located and consisted of the needle-like precipitates in a  $\beta$ -NiAl phase matrix. The needle-like phases contained low solubility elements (Cr, W and Ti) in the aluminides. The pores were distributed between the outer and the interdiffusion layers and were generated by the Kirkendall effect. Ni atoms diffused faster than Al atoms leading to the vacancies formation. The pores were formed as a result of their coalescence. The total coating thickness is 36 - 40  $\mu$ m (outer layer 18  $\mu$ m thick and interdiffusion layer 18-22  $\mu$ m thick) (Fig. 4).

The cross-section of the coating formed in the HTLA process is shown in Fig. 2b. Two layers were identified: the outer (A and B) and the interdiffusion one (C). The outer layer is the  $\beta$ -NiAl phase. The Al content 41.1 at. % and the Ni content 49.4 at. % on the



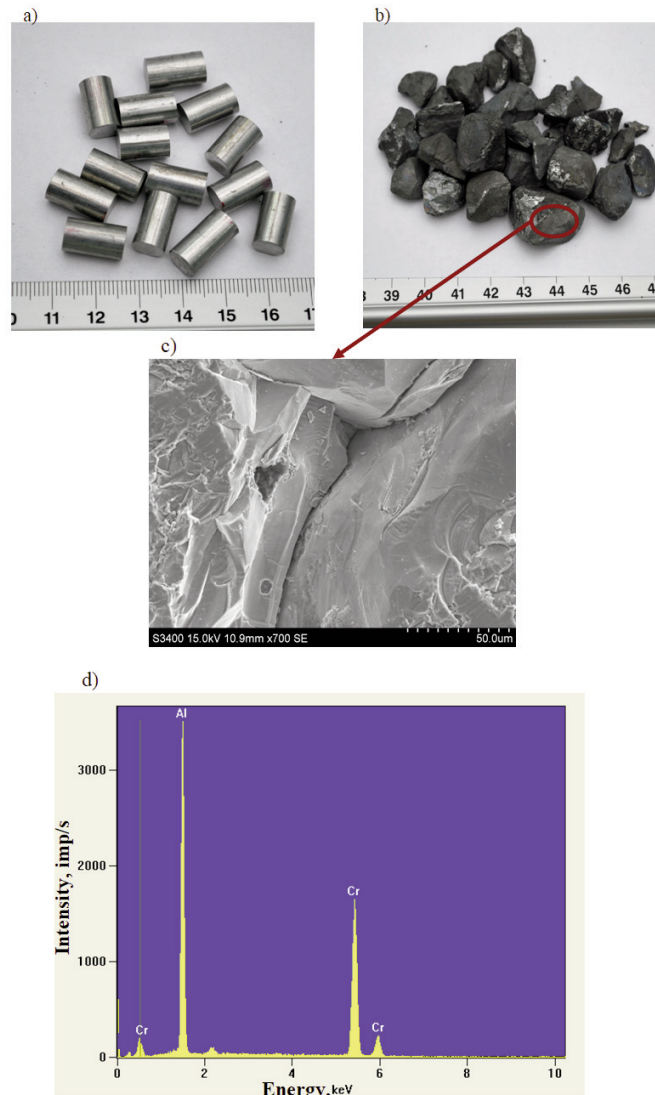


**Figure 1.** Aluminum 99.999 at. % (a), Al-Cr powder (b), surface morphology of the Al-Cr powder (c) and chemical composition of the Al-Cr powder (d)

distance from the surface 3-5  $\mu\text{m}$  (A) was found (Fig. 2-3b, Table 3). While the Al content 35.0 at. % and the Ni content 48.6 at. % on the distance from the surface 18-20  $\mu\text{m}$  (B) was proved. Cr and Co, which diffused from the substrate, were dissolved in the  $\beta$ -NiAl phase of the outer layer. The needle-like phases in the interdiffusion zone contained refractory elements: W, Cr and Ti. The total coating's thickness is 36 – 38  $\mu\text{m}$  (outer layer 18  $\mu\text{m}$  thick and interdiffusion layer 18-20  $\mu\text{m}$  thick) (Fig. 4).

Low activity aluminide coatings grow by the predominant Ni outward diffusion and consist of two layers. Ni diffuses outward and combines with Al to form  $\beta$ -NiAl phase in the external layer [13]. The external layer is a pure  $\beta$ -NiAl phase saturated with substrate elements which diffuse outwards from the

superalloy simultaneously with the Ni. The interdiffusion zone near the interface loses Ni. The loss of nickel from the superalloy results in the  $\beta$ -NiAl formation. The  $\beta$ -NiAl phase that formed in the interdiffusion zone has low solubility of the alloying elements of the superalloy. Therefore, these elements precipitate in the interdiffusion zone [13].

The formation mechanism of the HTHA type of coating could be explained by the predominant outward Ni diffusion from the substrate. The reaction front which is distributed in the outer layer surface receives Ni from the substrate and aluminium chlorides formed by the pack to form the  $\beta$ -NiAl compound. The area below the original surface of the alloy lost Ni due to its outward diffusion and received Al from the outer layer due to its inward diffusion.

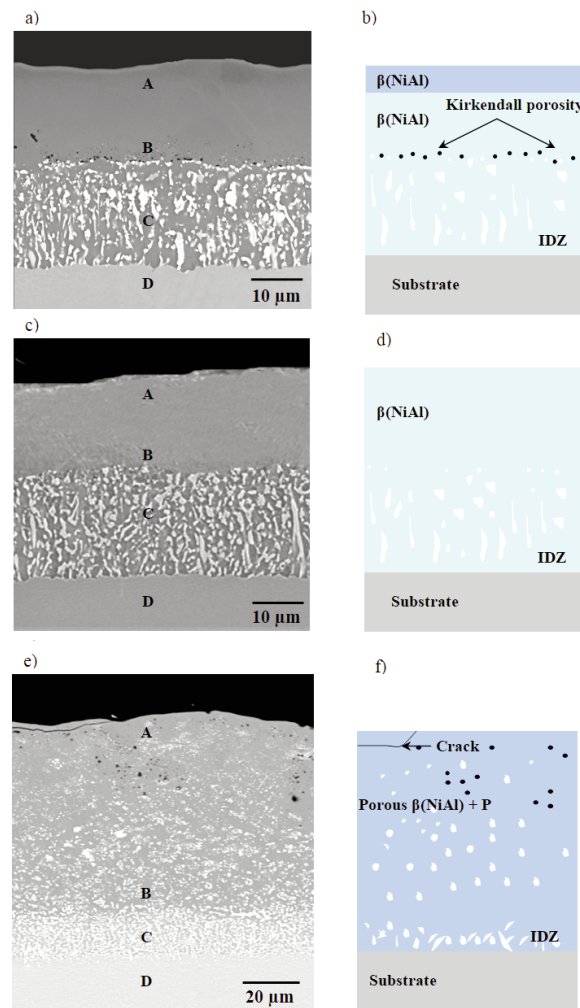


**Figure 2.** Cross-section microstructure and schematic representation of the coating formed by the HTHA process (a-b); HTLA process (c-d) and above-the-pack process (e-f)

**Table 3.** Chemical composition of zones in aluminide coatings (at. %) (Fig. 2)

Aluminizing process	Zone	Al	Ni	Cr	Co	Ti	W
HTHA	A	45.5±0.25	51.0±0.38	0.7±0.06	2.0±0.12	-	0.8±0.03
	B	34.5±0.24	52.1±0.39	4.9±0.09	7.1±0.15	1.0±0.04	0.4±0.03
	C	23.4±0.26	49.5±0.43	12.3±0.12	8.1±0.17	1.6±0.08	5.1±0.06
	D	12.8±0.24	63.9±0.49	9.5±0.12	8.9±0.19	2.3±0.05	2.6±0.05
HTLA	A	41.1±0.21	49.4±0.37	2.1±0.14	7.4±0.20	-	-
	B	35.0±0.20	48.6±0.35	5.8±0.12	9.9±0.19	0.7±0.10	-
	C	24.2±0.17	47.3±0.30	12.2±0.16	8.4±0.19	1.7±0.12	6.2±0.05
	D	12.1±0.23	62.8±0.36	9.9±0.17	9.7±0.20	3.1±0.13	2.4±0.05
above-the-pack	A	50.1±0.10	42.0±0.28	2.9±0.10	4.2±0.20	0.3±0.04	0.5±0.05
	B	42.6±0.20	42.8±0.31	5.0±0.12	5.8±0.22	1.0±0.09	2.8±0.06
	C	22.9±0.19	46.3±0.38	12.9±0.18	7.3±0.27	5.2±0.13	5.4±0.07
	D	12.3±0.18	63.9±0.46	10.0±0.18	9.1±0.31	2.6±0.13	2.1±0.07

The coating formed by the HTHA aluminizing consisted of two layers: the outer  $\beta$ -NiAl and the interdiffusion layer. No precipitates were found in the outer layer. This is different from that described in the literature (Fig. 5) [28]. Normally, precipitates of substrate elements are formed in the outer layer of the coating [28]. The obtained microstructure of the coating was similar to that formed by the HTLA aluminizing process.

There are differences between the low activity and high activity aluminide coatings [29]. The formed aluminide grains in the low activity coatings are larger than those in the high activity coatings, which means that there are fewer diffusion paths along the grain boundaries of the substrate. This means that Cr, Ti or W do not form precipitates in the outer layer. This may contribute to the improvement of the protection against oxidation and delay oxide spallation.

A cross-section of the coating formed in the above-the-pack process is shown in Fig. 2c. Two layers were identified: an outer (A and B) and the

interdiffusion one (C). The outer layer is  $\beta$ -NiAl phase. The Al content 50.1 at. % and the Ni content 42 at. % on the distance from the surface 3-10  $\mu\text{m}$  (A) was found (Fig. 2-3c, Table 3). While the Al content was 42.6 at. % and the Ni content 42.8 at. % on the distance from the surface 48-52  $\mu\text{m}$  (B) was proved. The outer layer is porous and contains precipitates of elements of the substrate that are not completely dissolved in the  $\beta$ -NiAl matrix. Porosity and segregation of precipitates can be detrimental for the alumina adherence during high temperature exposure of coated superalloy [29]. Needle-like precipitates in the  $\beta$ -NiAl matrix were found to be oriented perpendicular to the surface in the interdiffusion layer were revealed. The total coating thickness is 84  $\mu\text{m}$  (the outer layer 66  $\mu\text{m}$  thick and the interdiffusion layer is 18  $\mu\text{m}$  thick) (Fig. 4).

The Al and Ni distribution in the coating is shown in Fig. 3. The Al content decreases from the outer layer to the substrate. The concentration of Ni, on the other hand, remains in the outer layer almost constant.

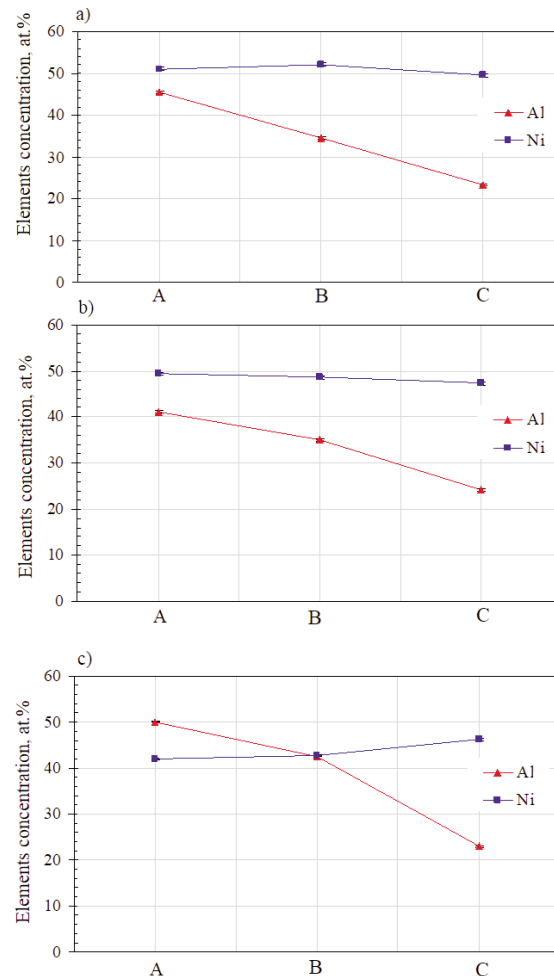


**Figure 3.** Al and Ni content in aluminide coatings zones formed by the HTHA process (a), HTLA process (b) and above-the-pack process (c)

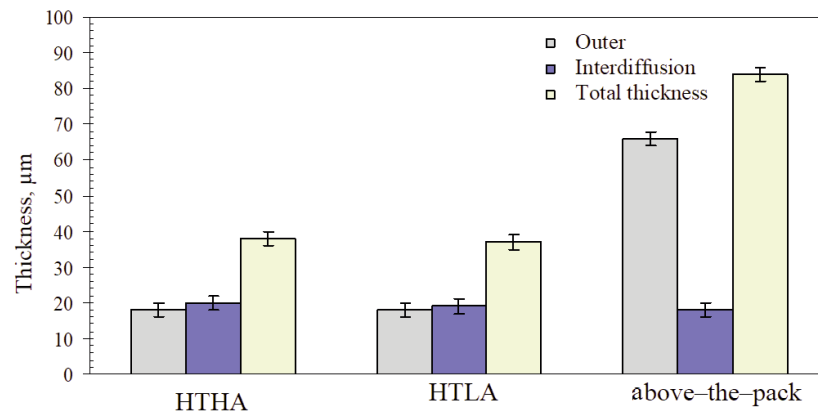


Figure 4. Thickness of aluminide layer formed by the HTHA process, HTLA process and above-the-pack process

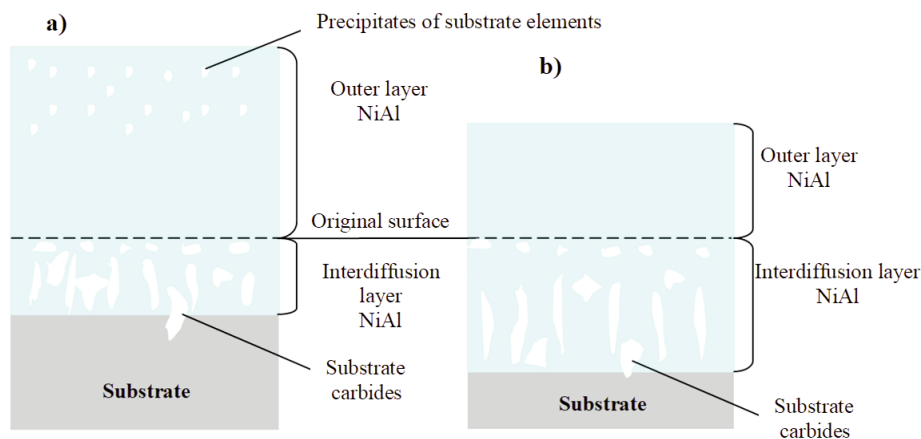


Figure 5. Schematic of the aluminide coating structure on nickel superalloy obtained by high (a) and low activity (b) process [28]

The average thickness of the coatings formed by different process is shown in Fig. 4. The maximum thickness was 84  $\mu\text{m}$ , for the coating formed by the above-the-pack process and the minimum thickness was 37  $\mu\text{m}$ , for the coating formed by the HTLA process.

An Al-rich hyperstoichiometric  $\beta$ -NiAl phase (Al > 50 at. %) was found in the coating produced in the above-the-pack process. Ni diffuses outwards in the bottom third of the interdiffusion zone, while Al diffuses inward in the top third of the coating [30]. Analysis of the microstructure showed precipitates in the outer layer. This was a consequence of the reduced Cr solubility in the hyperstoichiometric  $\beta$ -NiAl phase [31]. In contrast, the precipitates in the interdiffusion layer occurred due to the low solubility of elements of the substrate in the aluminide matrix. Moreover, the pores in the outer layer may be due to a high instantaneous flux of Al at the superalloy substrate/halides interface [32]. Body-centered cubic crystal structure of the  $\beta$ -NiAl phase was identified (Fig. 6).

### 3.2. Effect of aluminizing processes on the lifetime of coatings

The weight change curves of the superalloy with and without coating are shown in Fig. 7. The weight change of the uncoated superalloy decreased after only 30 h of oxidation. This is due to the insufficient protective properties of the oxides that formed on its surface. All coatings exhibited weight growth during first hours of oxidation which was caused by rapid oxides formation. The obtained results indicate that the worst oxidation resistance exhibits aluminide coatings formed by the above-the-pack process. The weight change reaches up to 0.3  $\text{mg}/\text{cm}^2$  during the 100 h of oxidation. Afterwards, the coating weight change starts to decrease slowly which indicates the onset of oxide scale spallation. Finally, the coatings weigh fell below its initial value in the 200 h. The coating formed by the HTHA process reached the maximum weight gain of 1.4  $\text{mg}/\text{cm}^2$  after 300 h of oxidation. Such weight change may be due to the very quick oxide formation. Thereafter, the weight change of the coating decreased and its weight fell below the

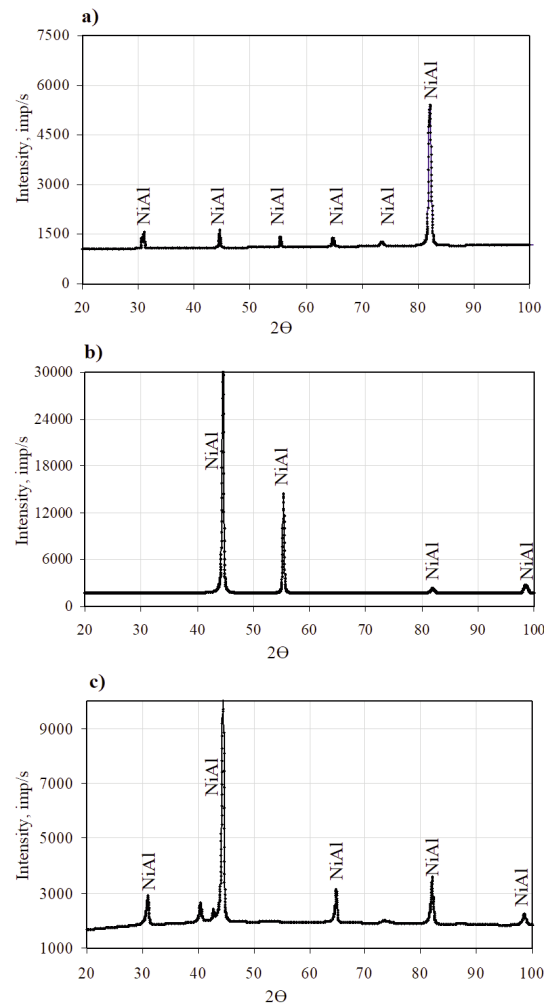


**Figure 6.** X-ray diffraction pattern of the coating formed by the HTHA process (a); HTLA process (b) and above-the-pack process (c)

initial value in 460 h. After 460 h of oxidation the weight change rapidly decreased, probably due to the inability of the oxides to reform after spallation. The weight gain of the coating formed by the HTLA process increased uniformly without fluctuations up to 1000 h of oxidation. This is due to the sufficient protective properties of oxides that formed on the surface of the coating.

The results of the investigation showed that the coatings formed by the HTLA process protect Mar-M247 superalloy up to 1000 h oxidation. Despite the fact that the coatings formed by the above-the-pack process were thicker and had a higher aluminium concentration than that formed by the HTLA process, the lifetime of the superalloy coated in the HTLA aluminizing process was longer than the superalloy coated by the above-the-pack process. Moreover, the lifetime of the superalloy coated in the HTLA process was longer than that of the superalloy coated by the single step HTHA process. The Al-Cr powder

contains 22 ppm sulphur in the above-the-pack aluminizing process [23,33-34]. Hydrogen could react with sulphur both in the powder and the aluminizing process to create the hydrogen sulphide gas. The hydrogen sulphide is supplied from the Al-Cr powder to the aluminide coating. The HTLA aluminizing process was realized without the Al-Cr powder. However, hydrogen reduced the surface before the aluminizing and removed sulphur from the surface. The aluminide coatings then have less sulphur than those deposited in the above-the-pack process. The purity of the coatings and their lifetimes are related. The removal of impurities in the HTLA aluminizing process ensures a “pure” outer layer. The clean aluminide coating may create the purer alumina oxide and prolong its lifetime. The oxidation resistance of the aluminide coating formed by the HTLA process makes it the preferred choice for gas turbine applications.

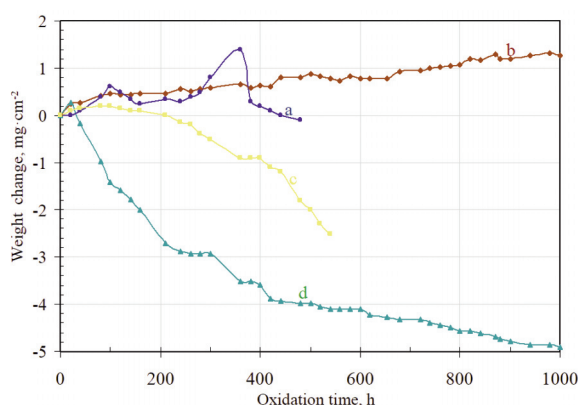


**Figure 7.** Weight change curves of the superalloy with coatings formed by the HTHA process (a); HTLA process (b); above-the-pack process (c) and uncoated superalloy (d)

#### 4. Conclusions

The aluminizing of the Mar-M247 superalloy by the HTHA, HTLA and above-the-pack processes led to formation of two layers (outer and interdiffusion layer) of the coatings. The outer layer of the coating formed by the above-the-pack process consisted of the  $\beta$ -NiAl phase with elements or compounds that diffused from the substrate, while the outer layer of the coatings formed by the HTHA and HTLA processes consisted of the pure  $\beta$ -NiAl phase. The predominant mechanism for the formation of the coatings during the HTLA and the HTHA processes was Ni outward diffusion.

In contrast, the predominant mechanism for the formation of the coating during the above-the-pack aluminizing process was Al inward diffusion. Aluminizing successfully improved the lifetime of the Mar-M247 superalloy. Despite the fact that the coating formed by the above-the-pack process was thicker and more Al concentration was found than in those formed by the HTLA process, the lifetime of the coated superalloy in the HTLA aluminizing process was higher than those coated in the above-the-pack process.

Moreover, the oxidation resistance of coated superalloy in the HTLA aluminizing process was higher than that of the one coated in the HTHA process. The removal of impurities in the HTLA aluminizing process ensured a “pure” outer layer. Clean aluminide coatings may create a purer alumina oxide and may prolong its lifetime.

#### Author contributions

*M. Zagula-Yavorska:* Conceptualization, Investigation, Methodology, Formal analysis, Writing–review & editing.

#### Conflict of interest

The author declare that they have no known competing financial interests or personal relationships that could have appeared to influence the work reported in this paper.

#### Ethical approval

This article does not contain any studies with human participants or animals performed by any of the authors. This study was done according to ethical standards.

#### Data availability

The data used to support the findings of this study are available from the corresponding author upon request.

#### References

- [1] M. Kassner, Fundamentals of creep in metals and alloys, Radarweg, 2009.
- [2] P. Ennis, Nickel-base alloys for advanced power plant components, Coal Power Plant Materials and Life Assessment, (2014) 147-167. <https://doi.org/10.1533/9780857097323.1.147>.
- [3] M.M. Barjesteh, S.M. Abassi, K. Zengeneh Madar, K. Shirvani, Creep rupture properties of bare and coated polycrystalline nickel-based superalloy Rene 80, Journal of Mining and Metallurgy, Section B: Metallurgy, 57 (3) (2021) 401 – 412. <https://doi.org/10.2298/JMMB201203036B>.
- [4] T. Pollock, S. Tin, Nickel-based superalloys for advanced turbine engines: chemistry, microstructure and properties, Journal of Propulsion and Power, 22(2) (2006) 361. <https://doi.org/10.2514/1.18239>.
- [5] E. Alabort, D. Barba, S. Sulzer, M. Lißner, N. Petrinic, R.C. Reed, Grain boundary properties of a nickel-based superalloy: characterisation and modeling, Acta Materialia, 151 (2018) 377-394. <https://doi.org/10.1016/j.actamat.2018.03.059>.
- [6] D. Szeliga, K. Kubiak, M. Motyka, J. Sieniawski, Directional solidification of Ni-based superalloy castings: thermal analysis, Vacuum, 131 (2016) 327-342. <https://doi.org/10.1016/j.vacuum.2016.07.009>.
- [7] A.M.S. Costa, E. Hawk, J. Dansbury, C.A. Nunes, G.E. Fuchs, Creep properties of directionally solidified Nb-modified Ni-Base superalloy, Mar-M247, Journal of Materials Engineering and Performance, 27 (2018) 5744–5751. <https://doi.org/10.1007/s11665-018-3699-6>.
- [8] S. Bose, High Temperature Coatings, Burlington, 2007.
- [9] B. Karpe, K. Prijatelj, M. Bizjak, T. Kosec, Corrosion properties of aluminized 16Mo3 steel, Journal of Mining and Metallurgy Section B-Metallurgy, 59 (1) (2023) 91-100. <https://doi.org/10.2298/JMMB220927008K>.
- [10] A. Karimzadeh, A. Sabour Rouhaghdam, Effect of nickel pre-plated on microstructure and oxidation behavior of aluminized AISI 316 stainless



- steel, *Materials and Manufacturing Processes*, 31(1) (2016) 87-94.  
<https://doi.org/10.1080/10426914.2015.1019091>.
- [11] S.J. Park, S.M. Seo, Y.S. Yoo, H.W. Jeong, H. Jang, Effects of Cr, W, and Mo on the high temperature oxidation of Ni-based superalloys, *Materials*, 12 (18) (2019) 2934. <https://doi.org/10.3390/ma12182934>.
- [12] M. Kopec, D. Kukla, X. Yuan, W. Rejmer, Z.L. Kowalewski, C. Senderowski, Aluminide thermal barrier coating for high temperature performance of MAR 247 nickel based superalloy, *Coatings*, 11 (1) (2021) 1-12.  
<https://doi.org/10.3390/coatings11010048>.
- [13] J. Romanowska, E. Dryzek, J. Morgiel, K. Siemek, Ł. Kolek, M. Zagula-Yavorska, Microstructure and positron lifetimes of zirconium modified aluminide coatings, *Archives of Civil and Mechanical Engineering*, 18 (2018) 1150-1155.  
<https://doi.org/10.1016/j.acme.2018.03.002>.
- [14] M. Zagula-Yavorska, J. Morgiel, J. Romanowska, J. Sieniawski, Microstructure and oxidation behaviour investigation of rhodium modified aluminide coating deposited on CMSX-4 superalloy, *Journal of Microscopy*, 261 (2016) 320-325.  
<https://doi.org/10.1111/jmi.12344>.
- [15] J. Romanowska, J. Morgiel, M. Zagula-Yavorska, J. Sieniawski, Nanoparticles in hafnium-doped aluminide coatings, *Materials Letters*, 145 (2015) 162-166.  
<https://doi.org/10.1016/j.matlet.2015.01.089>.
- [16] K. Beck, A.S. Ulrich, A.K. Czerny, E.M.H. White, M. Heilmaier, M.C. Galetz, Aluminide diffusion coatings for improving the peeling behavior of refractory metals, *Surface and Coatings Technology*, 476 (2024) 130205.  
<https://doi.org/10.1016/j.surfcoat.2023.130205>.
- [17] A. Kochmańska, P. Kochmański, Cyclic oxidation of slurry silicide-aluminide coatings formed on Ti-6Al-4V alloy, *Surface Engineering*, 39 (6) (2023) 738 – 750.  
<https://doi.org/10.1080/02670844.2023.2257856>.
- [18] K. Wierzbowska, A.E. Kochmańska, P. Kochmański, Resistance of aluminide coatings on austenitic stainless steel in a nitriding atmosphere, *Materials*, 15 (1) (2022) 162. <https://doi.org/10.3390/ma15010162>.
- [19] A.B. Smith, A. Kempster, J. Smith, Vapour aluminide coating of internal cooling channels, in turbine blades and vanes, *Surface and Coatings Technology*, 120–121 (1999) 112-117.  
[https://doi.org/10.1016/S0257-8972\(99\)00346-1](https://doi.org/10.1016/S0257-8972(99)00346-1).
- [20] R. Sitek, R. Molak, J. Zdunek, P. Bazarnik, P. Wiśniewski, K. Kubiak, J. Mizera, Influence of an aluminizing process on the microstructure and tensile strength of the nickel superalloy IN 718 produced by the Selective Laser Melting, *Vacuum*, 186 (2021) 110041.  
<https://doi.org/10.1016/j.vacuum.2020.110041>.
- [21] J. Benoit, K.F. Badawi, A. Malie, C. Ramade, Microstructure of Pt modified aluminide coatings on Ni-based superalloys without prior Pt diffusion, *Surface and Coatings Technology*, 194 (2005) 48–57.  
[https://doi.org/10.1016/S0257-8972\(03\)00871-5](https://doi.org/10.1016/S0257-8972(03)00871-5).
- [22] H. Zhang, Y. Liu, H. Su, W. Qu, H. Zhang, Y. Pei, S. Li, S. Gong, Effects of coating growth mode on the oxidation behavior of a hybrid Pt/Ru-modified aluminide coating at 1200 °C, *Corrosion Science*, 225 (2023) 111608.  
<https://doi.org/10.1016/j.corsci.2023.111608>.
- [23] B.M. Warnes, D.C. Punola, Clean diffusion coatings by chemical vapor deposition, *Surface and Coatings Technology*, 94-95 (1997) 1–6.  
[https://doi.org/10.1016/S0257-8972\(97\)00467-2](https://doi.org/10.1016/S0257-8972(97)00467-2).
- [24] V. Thongsiri, P. Visuttipitukul, S. Leelachao, Effect of heating rate on surface modification of Incoloy 825 by high activity pack aluminizing, *Materials Today: Proceedings*, 5 (2018) 9590–9594.  
<https://doi.org/10.1016/j.matpr.2017.10.142>.
- [25] M. Mojaddami, S. Rastegari, H. Arabi, H. Rafiee, Effect of heat treatment on coating microstructure applied by high activity diffusion process on IN738LC, *Surface Engineering*, 28 (2012) 772-777.  
<https://doi.org/10.1179/1743294412Y.0000000064>.
- [26] ASTM E3-11 (2017) Standard Guide for Preparation of Metallographic Specimens.
- [27] ASTM B487-20 (2020) Standard Test Method for Measurement of Metal and Oxide Coating Thickness by Microscopical Examination of Cross Section.
- [28] X. Montero, M.C. Galetz, M. Schütze, Low-activity aluminide coatings for superalloys using a slurry process free of halide activators and chromates, *Surface and Coatings Technology*, 222 (2013) 9-14.  
<https://doi.org/10.1016/j.surfcoat.2013.01.033>.
- [29] G.W. Goward, D.H. Boone, Mechanisms of formation of diffusion aluminide coatings on nickel-base superalloys, *Oxidation of Metals*, 3 (1971) 475–495.  
<https://doi.org/10.1007/BF00604047>.
- [30] A. Eslami, H. Arabi, S. Rastegari, Gas phase aluminizing of a nickel base superalloy by a single step HTHA aluminizing process, *Canadian Metallurgical Quarterly*, 48(1) (2009) 91–98.  
<https://doi.org/10.1179/cmq.2009.48.1.91>.
- [31] E. Pauletti, A. Monteiro d'Oliveira; Study on the mechanisms of formation of aluminized diffusion coatings on a Ni-base superalloy using different pack aluminization procedures, *Journal of Vacuum Science and Technology A*, 36 (4) (2018) 041504.  
<https://doi.org/10.1116/1.5026272>.
- [32] Z. Mutasim, J. Kimmel, W. Brentnall, Effects of alloy composition on the performance of diffusion aluminide coatings, *Proceedings of the ASME Turbo Expo*, 5 (1998). <https://doi.org/10.1115/98-GT-401>.
- [33] V. Genova, L. Paglia, G. Pulci, C. Bartuli, F. Marra, Diffusion aluminide coatings for hot corrosion and oxidation protection of nickel-based superalloys: effect of fluoride-based activator salts, *Coatings*, 11 (2021) 412. <https://doi.org/10.3390/coatings11040412>.
- [34] M.S. Priest, Y. Zhang, Synthesis of clean aluminide coatings on Ni-based superalloys via a modified pack cementation process, *Materials and Corrosion*, 66 (2015) 1111-1119.  
<https://doi.org/10.1002/maco.201408046>.



## ALUMINIZACIJA KAO METODA POBOLJŠANJA VEKA TRAJANJA LEGURE MAR-M247

M. Zagula-Yavorska

Tehnološki univerzitet u Žešovu, Odeljenje za nauku o materijalima, Fakultet mašinstva i aeronautike, Žešov, Poljska

### Apstrakt

Ekološki prihvatljivi procesi CVD aluminizacije visoke temperature visoke aktivnosti (HTHA) i visoke temperature niske aktivnosti (HTLA) realizovani su na podlozi superlegure Mar-M247 otporne na toplotu, koja se široko koristi u toplim delovima avionskih motora. Dodatno su analizirane komercijalne aluminidne prevlake nanosene u procesu aluminizacije gasnom fazom. Aluminizacija superlegure Mar-M247 pomoću HTHA, HTLA i gasnom fazom dovela je do formiranja dva sloja prevlaka. Spoljni sloj prevlake formiranog aluminizacijom gasnom fazom sastojao se od  $\beta$ -NiAl faze sa precipitatima, dok su se spoljni slojevi prevlaka formiranih procesima HTHA i HTLA sastojali od čiste  $\beta$ -NiAl faze. Aluminizacija je uspešno poboljšala vek trajanja superlegure Mar-M247. Uprkos činjenici da su prevlake formirane aluminizacijom gasnom fazom deblje i da sadrže veću koncentraciju aluminijuma nego premazi formirani HTLA aluminizacijom, vek trajanja prevučene superlegure bio je niži. Štaviše, otpornost na oksidaciju prevučene superlegure u procesu HTLA aluminizacije bila je bolja od one kod prevlaka formiranih HTHA aluminizacijom. Uklanjanje nečistoća u procesu HTLA aluminizacije obezbedilo je "čist" spoljni sloj prevlake. Čiste aluminidne prevlake mogu stvoriti čistiji aluminijum oksid i mogu produžiti njegov vek trajanja.

**Ključne reči:** HTLA proces; HTHA proces; Aluminizacija gasnom fazom; Vek trajanja

